AD-A041 737 NAVAL RESEARCH LAB WASHINGTON D C F/G 20/9

FORMATION AND ADIABATIC COMPRESSION OF REVERSED-FIELD THETA PIN--ETC(U)

FEB 77 D L BOOK, D HAMMER, P J TURCHI

UNCLASSIFIED NRL-MR-3491 NL

1 OF 1

AD A041737

END

DATE FILMED

8-77

AD A041737

12
B.S.

NRL Memorandum Report 3491

Formation and Adiabatic Compression of Reversed-Field Theta Pinches in Imploding Liners

D. L. Book, and P. J. Turchi
Plasma Physics Division

and

D. Hammer
University of California
Los Angeles, California

February 1977

NAVAL RESEARCH LABORATORY
Washington, D.C.

SECURITY CLASSIFICATION OF THIS PAGE (When Data Entered)

9

REPORT DOCUMENTATION PAGE

READ INSTRUCTIONS BEFORE COMPLETING FORM

1. REPORT NUMBER: NRL Memorandum Report 3491
2. GOVT ACCESSION NO.:
3. RECIPIENT'S CATALOG NUMBER:
4. TITLE (and Subtitle): 6 FORMATION AND ADIABATIC COMPRESSION OF REVERSED-FIELD THETA PINCHES IN IMPLODING LINERS.
5. TYPE OF REPORT & PERIOD COVERED: Interim report on a continuing NRL problem.
6. PERFORMING ORG. REPORT NUMBER:
7. AUTHOR(s): 10 D. L. Book, D. Hammer [redacted] P. J. Turchi
8. CONTRACT OR GRANT NUMBER(s):
9. PERFORMING ORGANIZATION NAME AND ADDRESS: Naval Research Laboratory, Washington, D.C. 20375
10. PROGRAM ELEMENT, PROJECT, TASK AREA & WORK UNIT NUMBERS: NRL Problem H02-37; ~~Project ERDA E (49-20)~~; 1009 ~~(81706)~~
11. CONTROLLING OFFICE NAME AND ADDRESS: Energy Research and Development Administration, Washington, D.C. 20545
12. REPORT DATE: 11 February 1977
13. NUMBER OF PAGES: 36
14. MONITORING AGENCY NAME & ADDRESS (if different from Controlling Office): 12 34p.
15. SECURITY CLASS. (of this report): UNCLASSIFIED
15a. DECLASSIFICATION/DOWNGRADING SCHEDULE:
16. DISTRIBUTION STATEMENT (of this Report): Approved for public release; distribution unlimited.

14 NRL-MR-3491

17. DISTRIBUTION STATEMENT (of the abstract entered in Block 20, if different from Report):

D D C
JUL 20 1977
C

18. SUPPLEMENTARY NOTES:
19. KEY WORDS (Continue on reverse side if necessary and identify by block number)

Adiabatic compression
Liners
Field reversal
Theta pinch

20. ABSTRACT (Continue on reverse side if necessary and identify by block number)

The formation and compression of e-beam-induced reversed-field theta pinch configurations is studied in an MHD treatment. Taking into account classical collisional resistivity plus anomalous resistivity derived from microinstabilities, it is shown that plasmas can be created with parameters suitable for liner compression experiments. Adiabatic compression of the quasi-equilibrium plasma/flux mixture is described using Lagrangian coordinates. Results are given for a sample (unoptimized) initial configuration. In the final state the average beta and the total D-T rate are ~ 10-20% of the values which would be obtained if all the compressional energy went into heating plasma.

approximately

DD FORM 1 JAN 73 1473 EDITION OF 1 NOV 65 IS OBSOLETE
S/N 0102-014-6601

SECURITY CLASSIFICATION OF THIS PAGE (When Data Entered)

251 950

LB

CONTENTS

FORMATION AND ADIABATIC COMPRESSION OF REVERSED-FIELD THETA PINCHES IN IMPLODING LINERS

I. Introduction

In the NRL "Captive Liner" concept,[1] a liquid metal liner implodes, heating a plasma by adiabatic compression to thermonuclear conditions. The liner, which is stabilized against Rayleigh-Taylor instability by rotation, rebounds after ignition, and the process is repeated cyclically.

One important problem under study is that of creating a suitable plasma in the interior of the device during each cycle prior to the implosion. Access to this region is possible only through the ends. The plasma must be sufficiently conducting ($T_e \geqslant 100$ eV) that a buffer magnetic field can be maintained between plasma and liner during the implosion. Further, since in most variants of the concept the implosion is quite slow ($V_L \leqslant 10^5$ cm/sec), the plasma-field configuration must be hydromagnetically stable over times $\geqslant 10^{-3}$ sec.

A promising candidate to meet these requirements is a reversed field theta pinch created by a rotating relativistic electron beam injected through the end of the system (see Fig. 1). This configuration has been demonstrated experimentally.[2] Reversed-field theta pinches (belt pinches) have displayed exceptional stability, apparently due to finite ion-gyroradius effects.[3]

To evaluate the prospects for e-beam-induced reversed-field configurations, several questions must be answered. One concerns the

Note: Manuscript submitted May 2, 1977.

scaling laws relating the e-beam parameters to those of the configuration (temperature, density and field profiles). Experiments now in progress at NRL are aimed at determining these laws. A second, the one addressed here, is related to the changes in the equilibrium resulting from compression, and their effect on the system's efficiency as a reactor. Logically, the next question (which has not yet been considered to any extent) would be the stability of such configurations. Presumably even initially stable configurations would become less so under compression as the density and field gradients steepen, and for any distribution a threshold must exist beyond which further compression produces unacceptable or even catastrophic destabilization. The characteristic time over which plasma confinement at maximum density must be maintained is $\sim a_o/V_L$, where a_o is the final (minimum) liner radius. This is substantially shorter than the total implosion time ($\sim$ 1 msec).

Throughout this paper we ignore end effects and azimuthal dependence, so that field and fluid quantities depend only on r. To give an idea of the sort of behavior to be expected, we begin by considering briefly the simplest ideal case, that of unmixed plasma and flux. In such an ideal final compressed configuration, the plasma, field and liner regions are distinct and sharply demarcated (Fig. 2). Pressure balance requires that

$$p_o = \frac{B_o^2}{2\mu_o} \quad . \tag{1}$$

where p_o is the plasma pressure and B_o the strength of the (uniform) buffer field. The region occupied by the reversed field is assumed vanishingly small. This is only valid if a relatively small fraction of the field lines of the total system are closed. Even in this limiting

case, the magnetic buffer zone must have a finite extent ($b_o > a_o$). Its thickness must be at least several ion gyroradii or mean free paths (if a cold background plasma is present) in order that the fluid picture be valid, and it must be thicker than the (as yet undetermined) region within which copious vapor or plasma from the liner is present. On the other hand, if it occupies a volume which is not small compared with the total compression volume, an intolerably large fraction of the system energy is diverted from the resulting plasma payload.

The D-T reaction rate divided by T^2 averagedover a Maxwellian distribution has a broad maximum at about 12 keV. Hence the payload state should ideally have a uniform temperature profile which attains this value at peak compression, as well as a uniform density. Given a configuration of this description, it is immediately possible to deduce the starting conditions (prior to compression) which will give rise to it. Let the precompression radius of the liner be called b_1, that that of the plasma-field interface a_1. Then conservation of flux implies

$$B_1 \, [b_1{}^2 - a_1{}^2] = B_o \, [b_o{}^2 - a_o{}^2] \tag{2}$$

Adiabatic compression of the plasma implies an initial pressure (assuming $\gamma = {}^5/_3$ and 2-dimensional compression) given by

$$p_1 = p_o(a_o/a_1)^{10/3} , \tag{3}$$

whence the magnetic field strength B_1 is found from

$$\frac{B_1{}^2}{2\mu_o} = p_1 \, . \tag{4}$$

conservation of total particle number implies a number density

$$n_1 = n_o(a_o/a_1)^2 , \tag{5}$$

which together with Eq. (3) gives a temperature

$$T_1 = T_o(a_o/a_1)^{4/3} \tag{6}$$

These relations suffice to determine the earlier state entirely, given the final values a_o, b_o, n_o and T_o (or B_o or p_o), and one other quantity, e.g., the compression ratio $\alpha = b_1/b_o$. For example, we have the results shown in Table I.

Table I

Quantity (units)	Final State	Initial State			
a (cm)	1.0	20.0	30.0	40.0	50.0
b (cm)	1.5	24.2	35.5	46.7	57.9
α	1.0	16.1	23.0	31.2	38.6
$n(cm^{-3})$	2.48×10^{18}	6.20×10^{15}	2.76×10^{15}	1.55×10^{15}	9.92×10^{14}
T(eV)	10^4	184	107	73.1	54.3
p (kbar)	39.3	1.81	0.468	0.180	0.085
B (kG)	10^3	6.78	3.45	2.14	1.47
ϵ	0.667	0.765	0.789	0.804	0.816

Here ϵ is the ratio of plasma energy to total energy,

$$\epsilon = \frac{a^2 \frac{3}{2} n k T}{a^2 \frac{3}{2} n k T + (b^2 - a^2) B^2/2\mu_o} . \tag{7}$$

It is clear that as we retreat to earlier and earlier initial states, the buffer region becomes thin relative to the plasma radius, although its absolute thickness is greater then in the final state.

The following phenomena act to prevent attainment of an ideal completely separated final plasma-field configuration: particle and thermal diffusion out of the plasma; inward diffusion of liner vapor and plasma; radiative cooling of the plasma; and initial deviations from complete separation due to transport processes and to the finite annular thickness of the injected e-beam. The last of these represents the particular concern of the present report. We develop a formalism suitable for determining the successive stages through which a mixed plasma-field configuration must pass under adiabatic compression, and apply it to a simple but realistic example.

The plan of the report is as follows. In Section II, we summarize the plasma processes (including anomalous heating) involved in producing the initial current distribution. In Section III we introduce a Lagrangian formalism to describe the compression history and apply it to a configuration derived in Section II. We conclude in Section IV with a discussion of our results and some recommendations for future study.

II. Formation of Field-Reversed Equilibrium

The experiments presently underway to study the production of a reversed-field configuration using relativistic electron beams are still in the preliminary stages. Therefore, a detailed characterization of the magnetic field and plasma pressure profile is not yet available. However, results to date[2] do indicate that the beam-plasma interaction is highly anomalous, since much higher plasma temperatures and net magnetic fields are observed than can be predicted on the basis of classical dissipation of the beam-induced azimuthal return current. For purposes of estimating the characteristics of the initial plasma that we might be able to produce using the Gamble II beam (electron energy 1.0 MeV, total current 1.5 MA, pulse length 70 nsec),[4] we have used the following model. A 1-5 kA/cm^2 beam is injected into a partially ionized hydrogen plasma, inducing an equal and opposite return current. This return current deposits energy in the plasma at a rate $\eta_{tot} j^2$, where η_{tot} is the classical resistivity due to Coulomb and electron-neutral collisions, plus the resistivity due to any instabilities which may be operative. When the beam pulse is over, the plasma must reach $\sim$ 100eV temperature, and the net current left behind in the system, equal to the net current in the system due to return current dissipation at the end of the beam pulse, must be large enough to produce the desired reversed-field plasma confinement geometry.

In order to determine the potential validity of this model, a computer code which follows the evolution in time of plasma density and temperature was used. This code, described elsewhere,[5] includes the principal ionization and radiation processes and an energy input term

ηj^2. Here η is determined at each instant of time from the plasma condition (η_e, T_e, T_i) for the various instabilities assumed to be present in a given run. Since the lower hybrid drift, ion acoustic, and electron electron two-stream instabilities are considered likely candidate sources of the anomalous heating in the experiments, we have tried resistivities derived for these three modes in various combinations and separately (but in all cases added to the classical resistivity).

The resistivity values used, expressed in ohm-cm, were

$$\eta_{c\ell} = 1.0\times10^{-2}\, T_e^{-3/2} \left[\ell n\, \Lambda + 1.4\times10^{-2}\, T_e\, (n_n/n_e)\right] ; \tag{8}$$

$$\eta_{\ell hd} = 4.3\times10^{-12}\, (B/n_e) \left[1 + (v_i/v_D)^2\right]^{-1} ; \tag{9}$$

$$\eta_{ia} = 1.2\times10^{6}\, n_e^{-1/2}, \quad v_D > v_{crit}$$
$$= 0 \text{ otherwise}; \tag{10}$$

$$\eta_{ee} = 3.3\times10^{19}\, J/n_e^{3/2}, \tag{11}$$

where $\ell n\, \Lambda$ is the Coulomb logarithm; n_n and n_e are neutral and electron number densities in cm^{-3}; B is magnetic field strength in kG; $\bar{v}_i = (2kT_i/M_i)^{1/2}$ is the ion thermal velocity in cm/sec; T_e and T_i are electron and ion temperatures in eV; v_D is the electron drift velocity,

$$v_D = 6.0\times10^{21}\, J/n_e \text{ cm/sec};$$

v_{crit}, the ion-acoustic cutoff, is given by

$$v_{crit} = 9.8\times10^{5}\, T_e^{1/2}\,]1.0 +$$
$$36.0\, (T_e/T_i)^{1/2} \exp(-.15 - 0.5\, T_e/T_i)] \text{ cm/sec}.$$

Here η_{cl} consists of Spitzer crossfield resistivity and an electron-neutral resistivity taken from Brown[6]; $\eta_{\ell hd}$ is a value obtained from Liewer[7]; η_{ia} is a value deduced from the experiment of Zavoiskii, et al.[8] and η_{ee} is from the parametric model of Papadopoulos.[9]

To summarize the results, by choosing the initial density appropriately, any one of the three anomalous resistivities acting alone was capable of producing the desired final plasma temperature for a beam current density in the range 3-5 kA/cm^2. (Classical resistivity alone required an order of magnitude more current density.) For illustrative purposes, we choose a case in which the electron-electron counter-streaming and ion acoustic modes are present. The results are shown in Fig. 3. The initial electron density was $5 \times 10^{13}/cm^3$, the neutral density (H) was $1.5 \times 10^{15}/cm^3$, and the initial temperatures ($T_i(0) = T_e(0)$ were 3eV. (The results are insensitive to $T_e(0)$, but do depend upon $n_e(0)$.) Figure 3a shows the electron and ion temperatures as a function of time during and shortly after the beam pulse. The initial rapid temperature rise is due to the small number of particles sharing the large energy input (the η's are all inversely proportional to n) at early time. This temperature rise causes rapid ionization (see Fig. 3b) which slows down the heating rate, causing the temperature to drop. Once the plasma is $>$ 90% ionized, energy input again goes into temperature rise instead of ionization, but now at a much lower rate. The heating of both electrons and ions in this case is a result of assuming the energy deposition is partitioned between electrons and ions as given by Liewer[7] for the two instability modes, respectively. Getting full ionization depends on the beam current density, as shown in Fig. 4 (the initial densities and

Since the L/R time and the implosion time (both of order msecs) are long compared with the magnetoacoustic scale, the plasma and field remain in quasi-equilibrium during the implosion. If we express the (azimuthal) current density in terms of B by Ampere's law,

$$\frac{dB}{dr} = -\mu_o j, \tag{14}$$

and combine this with (12) and (13), we find

$$\frac{dB}{dr} = -\mu_o \left(\frac{3p_p}{2\bar{\eta}\Delta t}\right)^{\frac{1}{2}} = \frac{1}{2}\left(\frac{3\mu_o}{\bar{\eta}\,\Delta t}\right)^{\frac{1}{2}} \left(B_o^{\,2} - B^2\right)^{\frac{1}{2}}, \tag{15}$$

where $\bar{\eta}$ represents the time-averaged value of η. Introducing scaled variables $b = B/B_o$ and $\rho = r/\Delta$ with $\Delta = \frac{1}{2}\left(\frac{3\mu_o}{\langle\eta\rangle\Delta t}\right)^{\frac{1}{2}}$, we have

$$\frac{db}{d\rho} = -\left(\langle\eta\rangle / \bar{\eta}\right)^{\frac{1}{2}} (1-b^2). \tag{16}$$

Here $\langle\bar{\eta}\rangle$ represents the spatial average of $\bar{\eta}$.

Depending on the exact microscopic model invoked in calculating the anomalous heating, we have

$$\eta / \langle\bar{\eta}\rangle = f\left[T, B, \frac{dB}{dr}, \text{etc.}\right]. \tag{17}$$

In the experiments to date, the induced current and heated plasma are located in the annular region originally occupied by the beam, and have radial profiles similar to the density profile of the latter. The observed[2] profiles tend to be broad, occupying a considerable fraction of the total system radius. It seems likely that the plasma profiles are determined mainly by that of the beam, not by the form of η. One

temperatures were held equal to those given above, and the same anomalous resistivity model was used in all cases).

For the case shown in Fig. 3, the plasma current dissipation, followed self-consistently in time, totals 10% at the end of the beam pulse, producing $500 A/cm^2$ net current. This is the current density which persists after the beam leaves the plasma. We assume the 1.5 MA Gamble II beam is used to form a 25 cm (average radius) annular rotating beam with a 10 cm thickness by passing through a cusp. If $V_\theta/V_z = 5$, the current density is $5\ kA/cm^2$. The net current found according to the calculation described above, $500\ A/cm^2$, is enough to reverse the 3 kG applied field on axis in this case. This configuration has a classical L/R time of 30 msec for T = 100 eV. Since the current density is an order of magnitude smaller than when the beam was present, it is reasonable to expect the microinstabilities causing anomalous resistivity will be absent during this time.

The beam-induced return-current heating therefore takes place principally over the lifetime Δt of the rotating e-beam, of order 100 nsec. The plasma pressure as a function of position is thus given by

$$\frac{3}{2}\ p \approx \int_0^{\Delta t} \eta j^2\ dt, \tag{12}$$

where η includes both the classical and anomalous resistivity. After a time on the order of a new magnetoacoustic transit times across the radius R_o of the system (a few μsec), pressure balance is established:

$$p_p + \frac{B^2}{2\mu_o} = \frac{B_o^{\ 2}}{2\mu_o} = \text{const.} \tag{13}$$

thus concludes that η cannot have a very strong dependence on position. This is in contrast with the situation in collisionless-shock-heating theta pinch experiments (with and without bias fields)[10] in which the current profile is established through microscopic processes and tends to be of order c/ω_{pi} (initially 1-2 orders of magnitude smaller than the radius for the parameters we are considering).

Thus whenever η is large enough to make Δ comparable with the system radius, it is reasonable to approximate $\eta = \eta_o$ = constant, whence from (16) $b = - \sin \rho$, or

$$B(r) = - B_o \sin \left(\frac{r}{\Delta}\right), \tag{18}$$

where $\Delta = R_o/\pi$. From Eq. (18) it follows that the plasma pressure $p(r)$ vanishes at $r = r$ and $r = R_o$, consistent with the requirements that the density vanish on axis and the temperature vanish at the liner. Figure 5 shows the field and pressure profiles associated with Eq. (18).

Another simple solution results if we assume

$$\eta \propto p_p = 2\mu (B_o{}^2 - B^2) \tag{19}$$

For this model, Eq. (16) becomes

$$\frac{dB}{dt} = - \mu\, j = \text{const.} \tag{20}$$

Thus the current density is uniform, B varies linearly,

$$B = B_o (2r-R_o)/R_o , \tag{21}$$

and the pressure profile is parabolic:

$$p = (2B_o^2/\mu)(r/R_o)(1-r/R_o). \tag{22}$$

We refer to these two models as the sinusoidal and uniform current approximations. In spite of the difference in the assumptions on the functional form of η, they are qualitatively (and quantitatively) very similar. The numerical results described in the next section depend only weakly on which is studied. Again, this tends to justify our belief that the complicated physics embodied in the definition of η is less important then its average magnitude. This is fortunate, as none of the resistivities in Eqs. (8-11) is well approximated by a constant or by Eq. (19).

In the high current density limit for which ionization occurs rapidly and requires only a small portion of the total energy deposited by resistive heating, the electron density follows the initial neutral density distribution. With uniform initial gas fill the ion acoustic mode then provides a sinusoidal current distribution self-consistently. Electron-electron two-stream and lower hybrid drift instabilities provide current distributions that are intermediate between the sinusoidal and uniform current models.

III. Adiabatic Compression

Let the system be compressed by reducing the liner radius from R_o to R. A differential element originally at r_o is displaced to a new position $r(r_o)$, where $0 \le r \le R$, and undergoes a volume compression $w(r_o)$:

$$w(r_o) = \frac{2\pi r_o dr_o}{2\pi r dr} . \tag{23}$$

Since the magnetoacoustic transit time is much shorter than the compression time, the system remains in pressure balance:

$$\frac{\partial p}{\partial r} = \frac{\partial p}{\partial r_o} = 0 , \tag{24}$$

where

$$p = p_M(r) + p_P(r) \tag{25}$$

is the sum of magnetic and plasma pressures.

Using the adiabatic laws with $\gamma = 2$ and $\gamma = 5/3$, respectively, yields

$$p_M = p_{M_o} w^2 ; \tag{26}$$

$$p_P = p_{P_o} w^{5/3} . \tag{27}$$

Hence by the definition of the initial local beta,

$$\beta_o(r_o) = p_{P_o}/p_o , \tag{28}$$

$$p = p_o [(1-\beta_o) w^2 + \beta_o w^{5/3}] , \tag{29}$$

where p_o is the initial pressure. From (24) and (29) we find

$$\frac{dw}{dr_o} = \frac{w(1-w^{-1/3})}{2(1-\beta_o) + 5/3 \beta_o w^{-1/3}} \frac{dp_{P_o}}{dr_o} . \tag{30}$$

By the frozen-in condition, if p_{p_o} vanishes at $r_o = 0$, then $p_p(r_o = 0)$ vanishes at all subsequent stages. Furthermore, $r(0) = 0$ by symmetry. We can parametrize the compressional process by the volume compression w_o of a plasma-free differential element of the system, $w_o = w(0)$.

The instantaneous radial displacement r of a differential element is related to the original position r_o by Eq. (23), or equivalently,

$$\frac{dr^2}{dr_o} = 2r_o \frac{rdr}{r_o dr_o} = \frac{2r_o}{w} . \tag{31}$$

Equations (30) and (31), together with the initial conditions $r(0) = 0$, $w(0) = w_o$, can be integrated numerically to provide a parametric definition of the function $w(r)$. The compressed-state radius follows from

$$R = r(R_o). \tag{32}$$

Instead of w_o, it is now convenient to use as a measure of the compression the inverse scaled system radius,

$$\alpha = R_o/R, \tag{33}$$

defined parametrically by (32).

A knowledge of $w(r) = w\,[r(r_o)]$ suffices to generate profiles of density, temperature, pressure and magnetic field strength:

$$n(r) = n_o(r_o)\, w; \tag{34}$$

$$T(r) = T_o(r_o)\, w^{2/3} ; \tag{35}$$

$$p_P(r) = p_{P_o}(r_o)\, w^{5/3} \;; \tag{36}$$

$$B(r) = B_o(r_o)\, w \,. \tag{37}$$

The ratio of plasma to total energy is

$$\epsilon = \frac{W_P}{W_M + W_P} = \frac{\frac{3}{2}\int_o^R r dr P_P(r)}{\int_o^R r dr [p_M(r) + \frac{3}{2} p_P(r)]}$$

$$= \frac{\frac{3}{2}\int_o^{R_o} r_o dr_o \, \beta_o \, w^{2/3}}{\int_o^{R_o} r_o dr_o \, [(1-\beta_o)\, w + \frac{3}{2}\beta_o w^{2/3}]} \,. \tag{38}$$

Figure 6 shows how ϵ and the average beta vary with α, assuming the uniform current model. In Fig. 7, a log-log plot of p vs. α^{-2} is shown. It is clear that the compression is well approximated by an adiabatic law.

$$p\alpha^{2\gamma_{eff}} = \text{const}, \tag{39}$$

with $\gamma_{eff} = 1.82$. For the sinusoidal model, the corresponding value of γ_{eff} is 1.85.

In the course of the implosion, the plasma is more readily compressed than is the magnetic flux. As a result, the "field-rich" region

region occupies an ever-increasing share of the total volume at the expense of the "plasma-rich" region. This is reflected in the marked reduction in ϵ and the average β, and is accompanied by an inward shift in the relative position of the field-reversal point.

Assuming a system which operates with a compression value $\alpha = 35$, we find a final state with $\epsilon = .30$.

For this state the radial profiles are depicted in Figure 8. Assuming uniform initial density and writing $p = nkT$, we can calculate the radial dependence of n and T separately, as shown. Note the general steepening of all gradients, a feature which may be expected to reduce the margin of MHD stability initially present.

Thus far we have worked in terms of scaled variables. If we specify the final conditions according to

$$B_{max} = 1 \text{ MG} ,$$

and correspondingly,

$$p = \frac{B^2_{max}}{2\mu_o} = 39 \text{ kbar},$$

and select T_{max} to be in the range of thermonuclear interest, then we can calculate the total D-T power rate:

$$P_{D-T} = 2.8\text{x}10^{-24} \left\langle n^2 T^{-2/3} \exp(-19.94T^{-1/3}) \right\rangle_{ave} \text{W/cm}^3, \qquad (40)$$

where T is temperature in keV and the average is carried out over the plasma cross-section. If this is scaled by P^{opt}_{D-T}, the power rate which would be obtained if all the compressional energy resided in a plasma of uniform pressure 39 kbar and temperature equal to T_{max}, and the results

plotted against temperature, Fig. 9 is obtained. The curve peaks at approximately 15 keV (slightly higher than the maximum of the unaveraged D-T rate for constant plasma pressure), with values of order 10% of the optimum ones.

If the same scaling is used with the average of the bremsstrahlung power rate,

$$P_{Br} = 5.3\text{x}10^{-31} \langle n^2 T^{\frac{1}{2}} \rangle \sim p^2 \langle T^{-\frac{1}{2}} \rangle , \qquad (41)$$

Fig. 10 results. Evidently, for a given pressure the optimum working temperature lies somewhere above 15 keV. Lower temperatures (which are naturally easier to obtain) penalize the system in terms both of yield and radiation losses.

IV. Conclusions

In this paper we have discussed (1) the form of the reversed-field equilibrium configuration induced by a rotating e-beam and (2) how it changes under adiabatic compression. In view of the idealizations employed, our conclusions are qualitative and somewhat tentative. Nevertheless, they bear closely on the question of utilizing the reversed-field theta-pinch in liner reactor designs, and so are of practical importance.

First, we have observed in Section II that the initial reversed-field configuration appears to be determined principally by the pulse length, current density and radial dimensions of the relativistic e-beam. (Confirmation of this will have to await further experimental work.)

Our heating calculations show that the initial configuration does not depend strongly on the details of the heating process, i.e., the anomalous resistivity mechanism(s). Further, the final state (for a specified ϵ) of the reversed-field equilibrium under compression is insensitive to the exact shape of the initial profiles (Section III).

The second conclusion is that, without optimization of the initial configuration, the reversed-field theta pinch leads to average values of beta which, though substantial, are considerably less then unity. Moreover, because of the nonlinear functional dependence of the D-T power rate, the yield is even further below the optimum which would be achieved if only uniform plasma were compressed. Against this must be balanced the consideration that may well be possible to create sharper profiles with initial ϵ higher than that used in the present calculations (.75). Further, some of the flux at large radii is actually lost by diffusion into the liner. Although such losses are in general undesirable, it is important not to count the energy so removed twice-if flux is lost by diffusion, the average beta must increase correspondingly.

We note that the formalism we have developed is appropriate for calculating the adiabatic radial compression of an arbitrary reversed-field theta pinch. It may also be used directly to obtain integrals (in a linear approximation) of total D-T yield, radiation losses, particle and heat loss and magnetic flux diffusion, as in the example described above. Evidently there is no need to restrict consideration to initial states for which an analytic representation is available.

The present formalism will be applied in existing codes modeling the self-consistent dynamics of imploding liners. We have shown that the pressure of such a configuration is well described by an ideal-gas adiabatic law with an effective γ (ratio of specific heats) which is weakly dependent on the shape. The successive states so generated can then be made the object of a study of both hydromagnetic and micro-instabilities. As mentioned previously, both types depend sensitively on the form of field and plasma profiles. If the initially broad field reversal region becomes of order c/ω_{pi}, collective phenomena resembling those in collisionless shocks will probably occur, giving rise to an enhanced resistivity ν^*.

In order that the profiles calculated according to the assumption of adiabatic compression not be smeared out by diffusion, we must have

$$Dt_o < \Delta^2, \tag{42}$$

where D is the radial diffusion rate, $t_o = a_o/V_L$ is the characteristic dwell time, and Δ is the sheath thickness. In the final state the ions are strongly magnetized ($w_{ci}\tau_i \sim 10^4$, where τ_i is the ion collision time). Thus we can write

$$D = \nu^* r_i^2 ,$$

where $r_i = 4.5T^{\frac{1}{2}}/B$ cm is the ion gyroradius (here T is in keV, B in kG). Condition (42) then becomes

$$\nu^* < 0.05 \, (\Delta/a_o)^2 \, a_o V_L \, B^2/T. \tag{43}$$

Taking $T = 10$ keV, $B = 1$ MG, $a_o = 1$ cm and $V_L = 3\text{x}10^4$ cm/sec yields

$$\nu^* < 1.5 \times 10^8 \, (\Delta/a_o)^2 \ \text{sec}^{-1}. \tag{44}$$

If $\Delta/a_o = 0.1$, $\nu^* < 1.5 \times 10^6$ sec^{-1} must hold. By comparison, the classical ion collision rate with these parameters and $n = 2.5 \times 10^{18}$ cm^{-3} is $\nu_{cl} \approx 9\text{x}10^5$ sec^{-1}. Thus if the collision rates in the final plasma state are classical, our model should be adequate to provide an indication of the plasma/field configuration.

ACKNOWLEDGEMENT

This work was supported in part by ONR and ERDA.

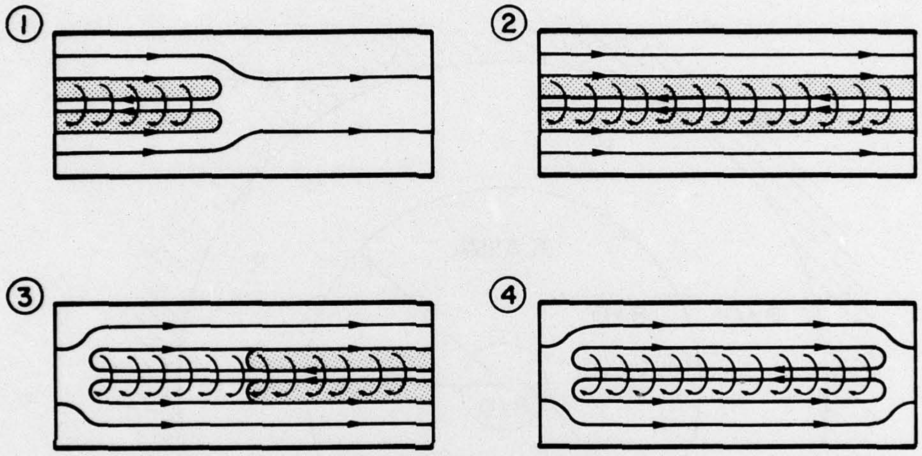

Fig. 1 — Formation of a reversed-field-theta-pinch by a rotating relativistic e-beam. The beam enters a drift tube filled with cool gas or plasma (1), reversing the field on axis. The beam-induced return current decays owing to the initial high plasma resistivity, heating the plasma (2). The plasma conductivity thus increases, so that when the beam exits (3), a plasma current is induced in the same sense as that of the beam. This persists (4) for times long compared with the beam lifetime, since the plasma has become hot and highly conducting.

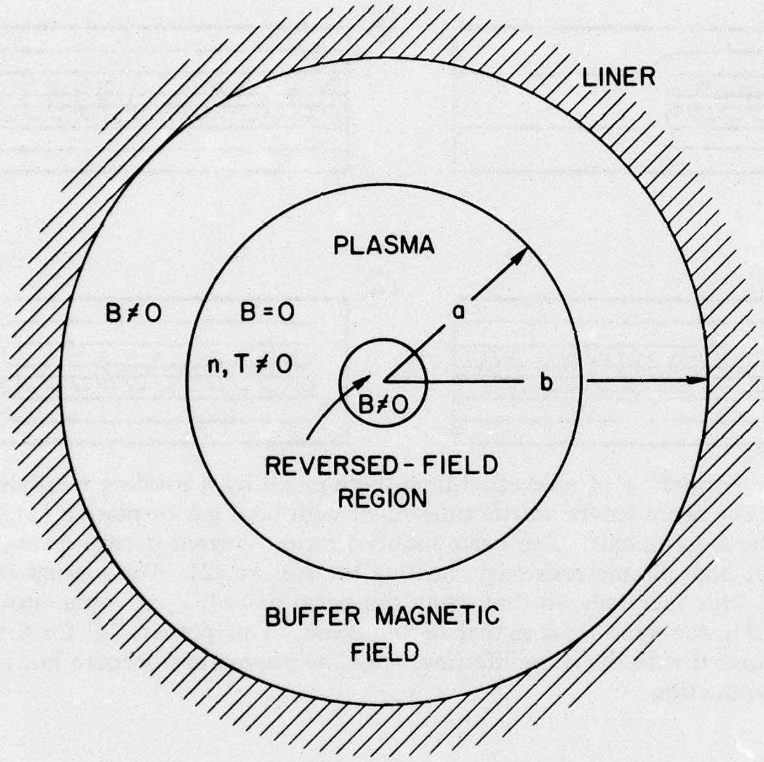

Fig. 2 — Schematic of one-dimensional (no Z or θ dependence) reversed-field theta pinch configuration with unmixed field and plasma

(a)

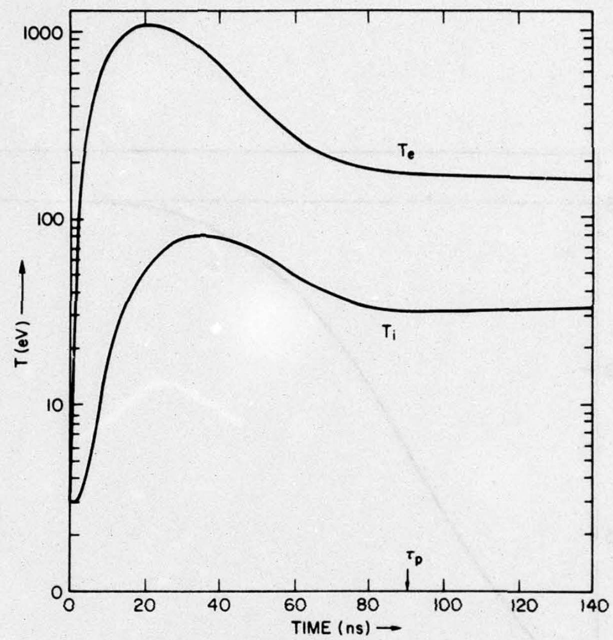

(b)

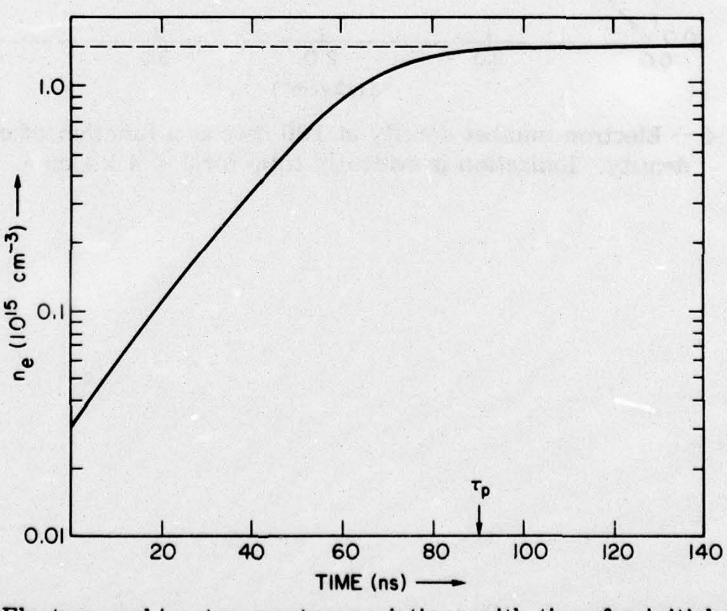

Fig. 3 — (a) Electron and ion temperature variations with time for initial electron density $n_e = 3 \times 10^{13}$ cm^{-3}, neutral H density $n_n = 1.5 \times 10^{15}$ cm^{-3} (20 m torr), temperatures $T_i = T_e =$ keV, current density J = 5 kA/cm^2, due to the action of classical, electron-electron two-stream and ion-acoustic resistivities. The nominal beam lifetime τ_p is 90 nsec. (b) Electron density as a function of time for the same case.

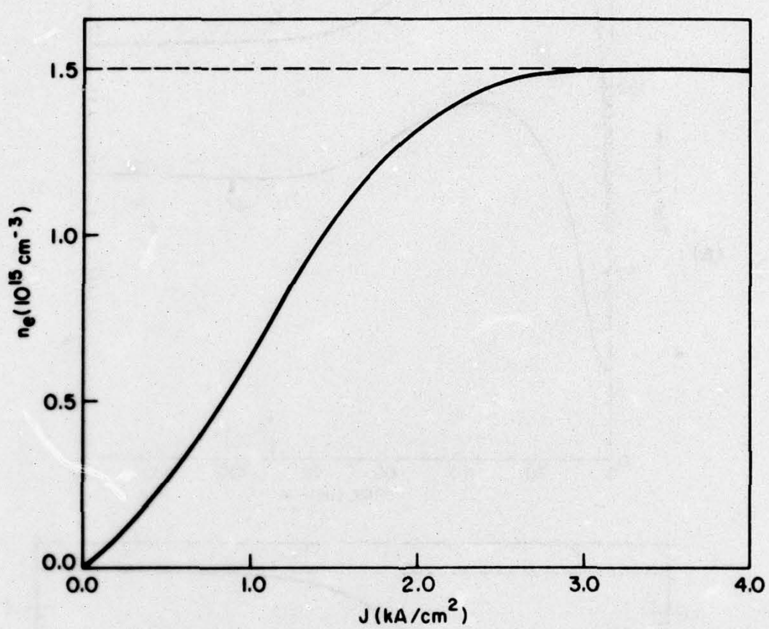

Fig. 4 — Electron number density at 100 nsec as a function of current density. Ionization is evidently total for J $\gtrsim$ 4 kA/cm^2.

(a)

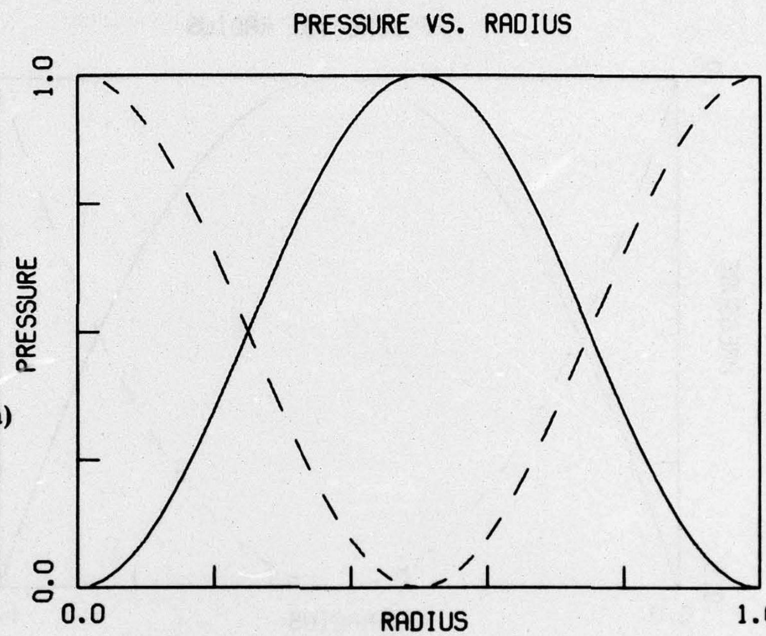

(b)

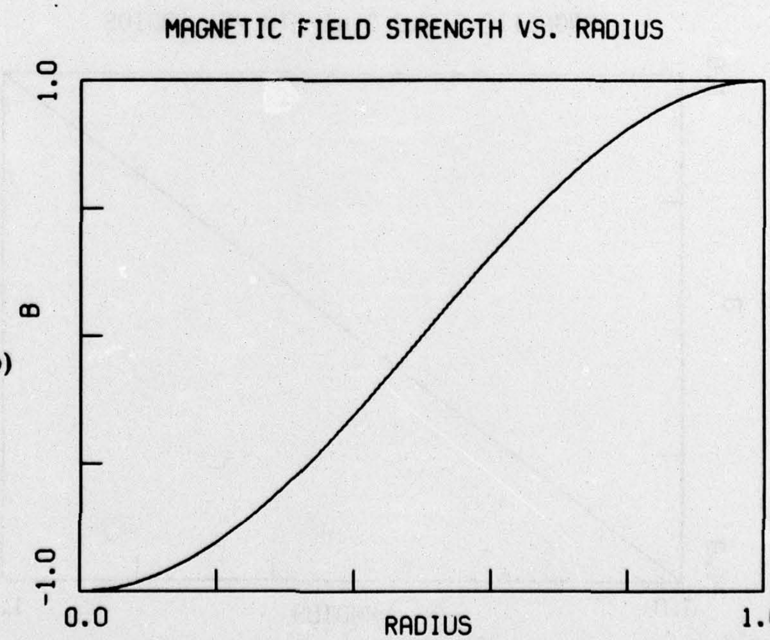

Fig. 5 — Initial pressure and field profiles. (a) Plasma (solid curve) and magnetic (broken curve) pressures for the sinusoidal case, and (b) magnetic field strength for the same case. (Continues)

(c)

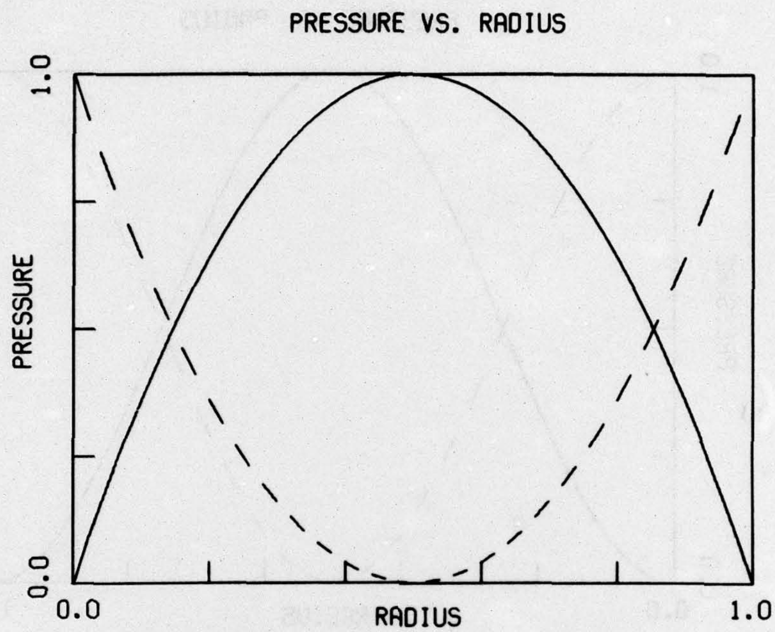

(d)

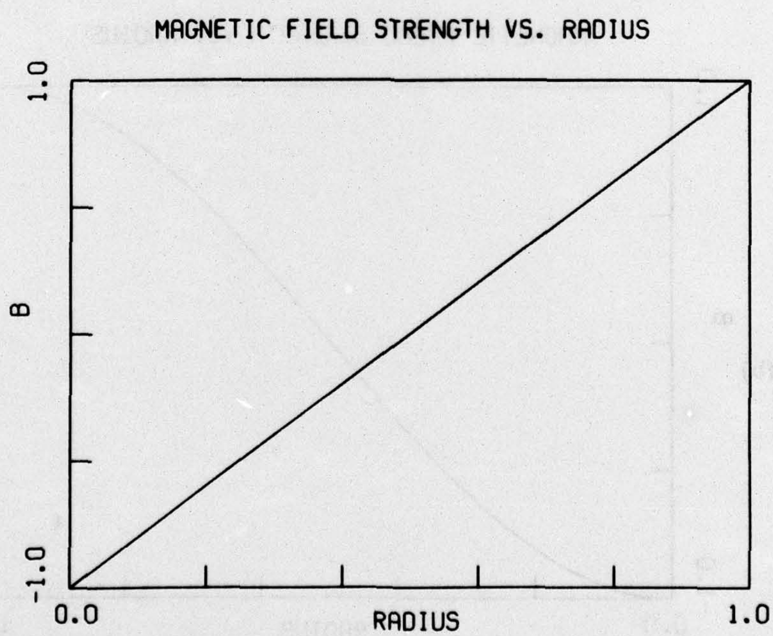

Fig. 5 (Continued) — Initial pressure and field profiles (c) plasma and magnetic pressures for the uniform current case, and (d) corresponding field profile.

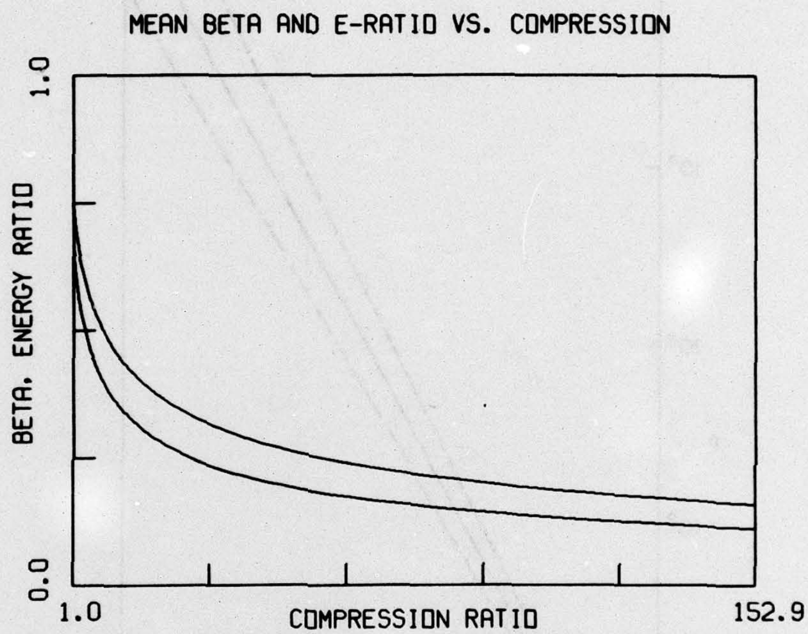

Fig. 6 — Ratio ϵ of plasma energy to total energy (upper trace) and average beta (lower trace) as a function of α, the radial compression factor, for the uniform current case

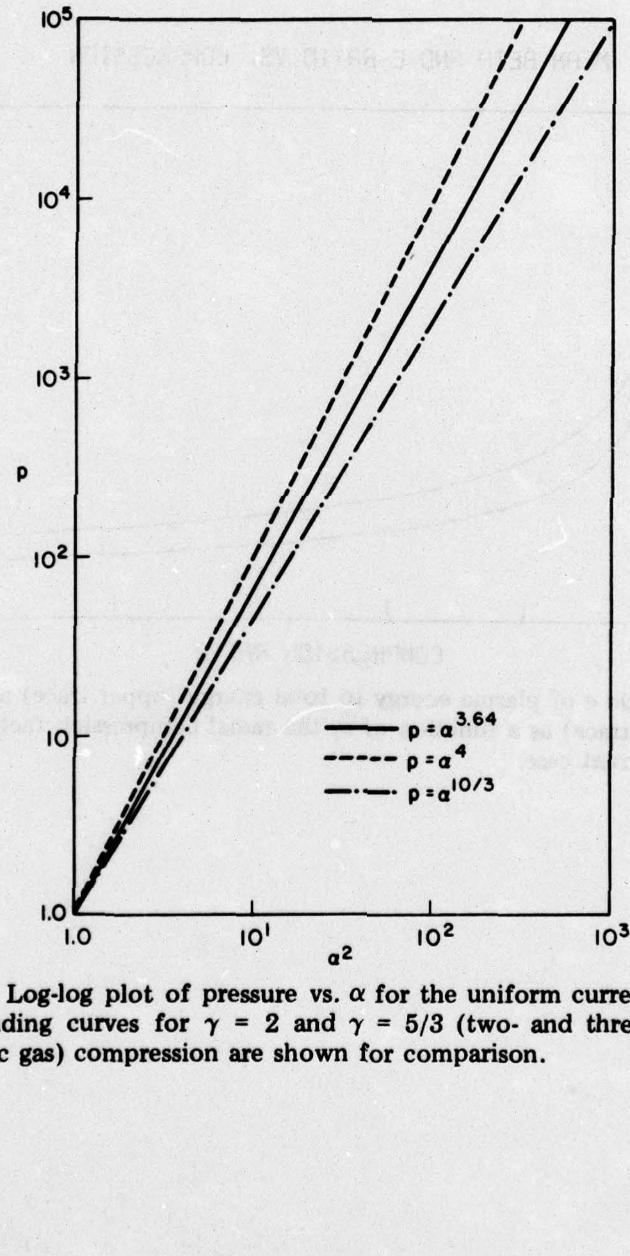

Fig. 7 — Log-log plot of pressure vs. α for the uniform current case. The corresponding curves for $\gamma = 2$ and $\gamma = 5/3$ (two- and three-dimensional polytropic gas) compression are shown for comparison.

(a)

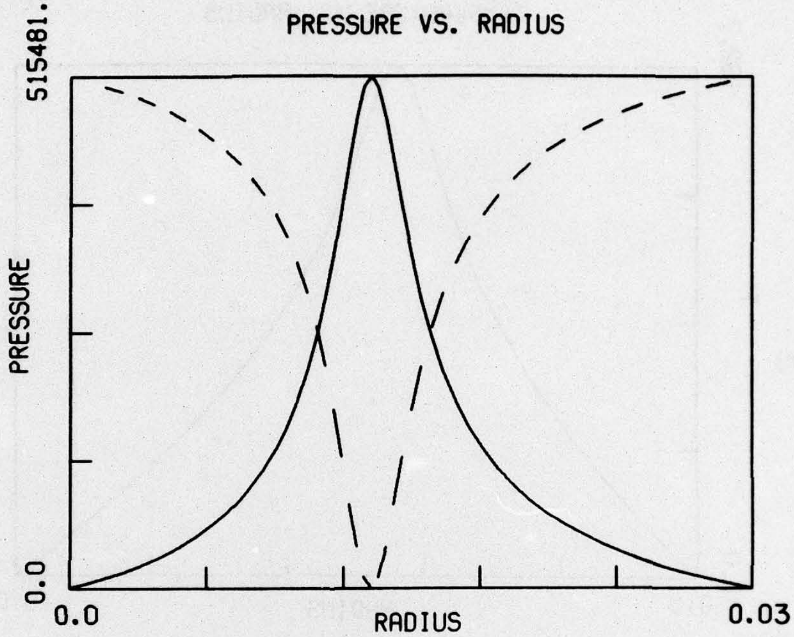

(b)

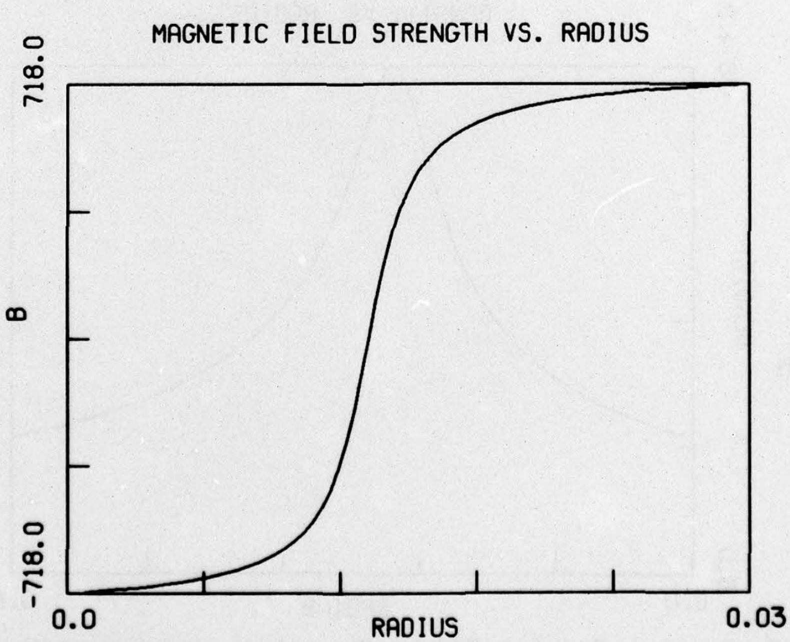

Fig. 8 — Radial profiles for the uniform current case with $\alpha = 35$ ($\epsilon \approx 0.3$), assuming an initially uniform density profile (cf. Fig. 5): (a) plasma (solid curve) pressures and (b) magnetic field (Continues)

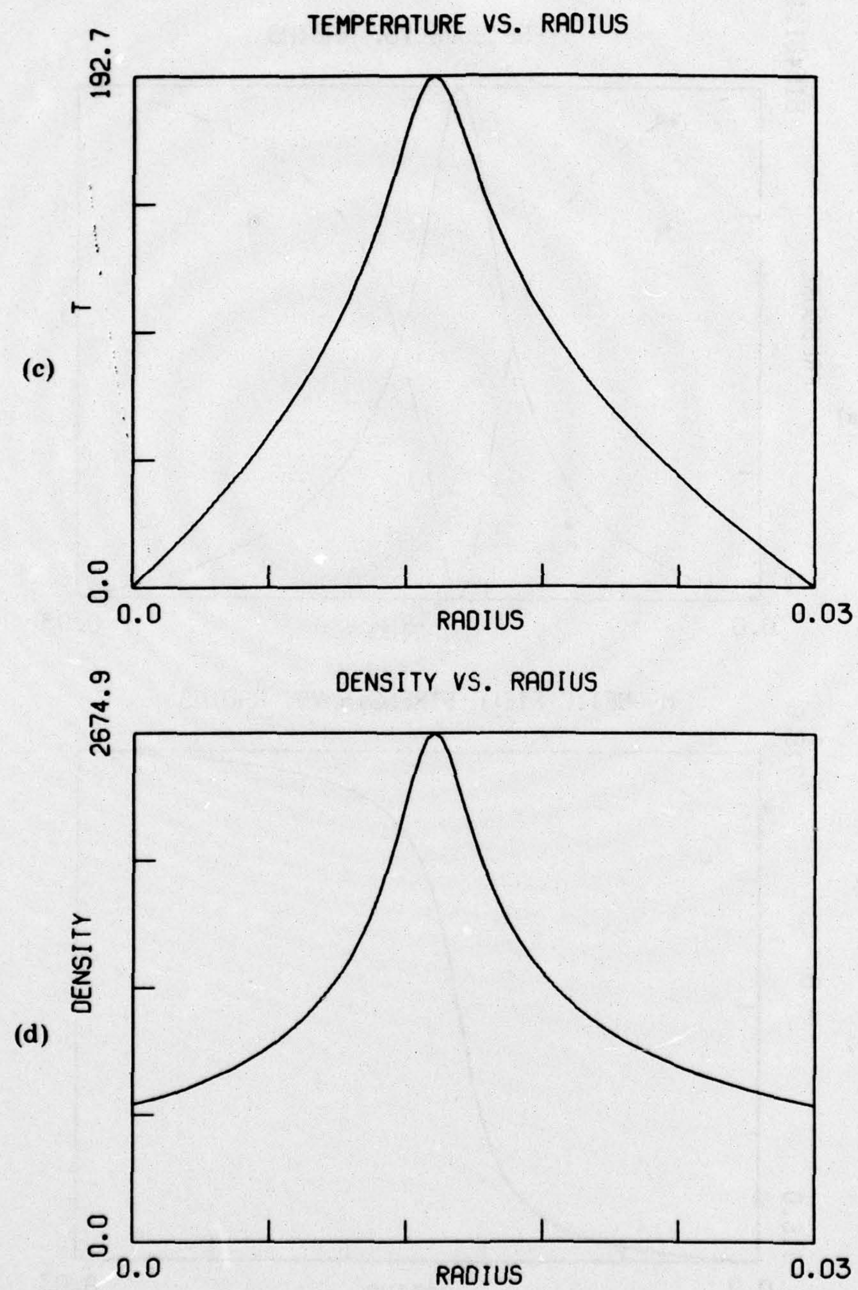

Fig. 8 (Continued) — Radial profiles for the uniform current case with α = 35 ($\epsilon \approx 0.3$), assuming an initially uniform density profile (cf. Fig. 5): (c) temperature, and (d) density

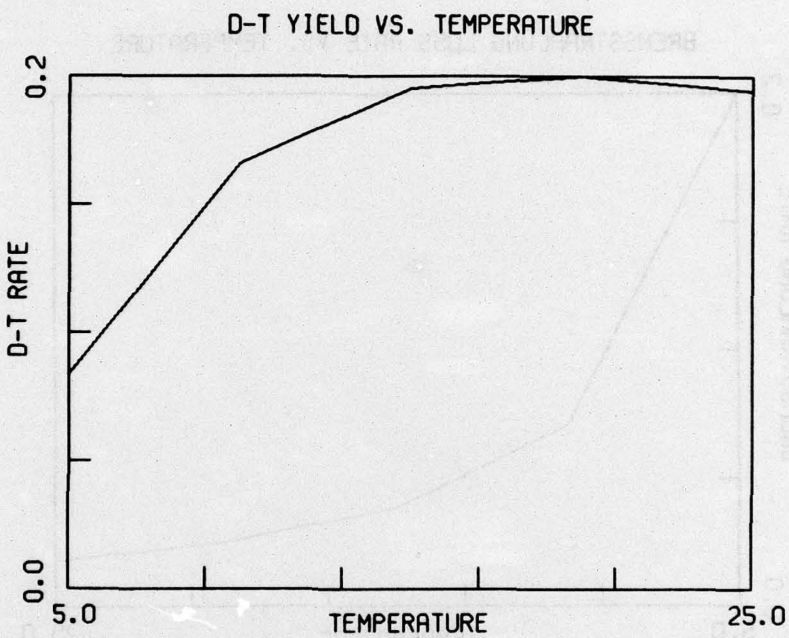

Fig. 9 — Total D-T power rate for the state shown in Fig. 8, scaled by the power which would be obtained if all the compressional energy had gone its plasma heating. The values shown are for temperature T = 5, 10, ..., 25 kev, assuming constant pressure and Maxwellian ion distributions.

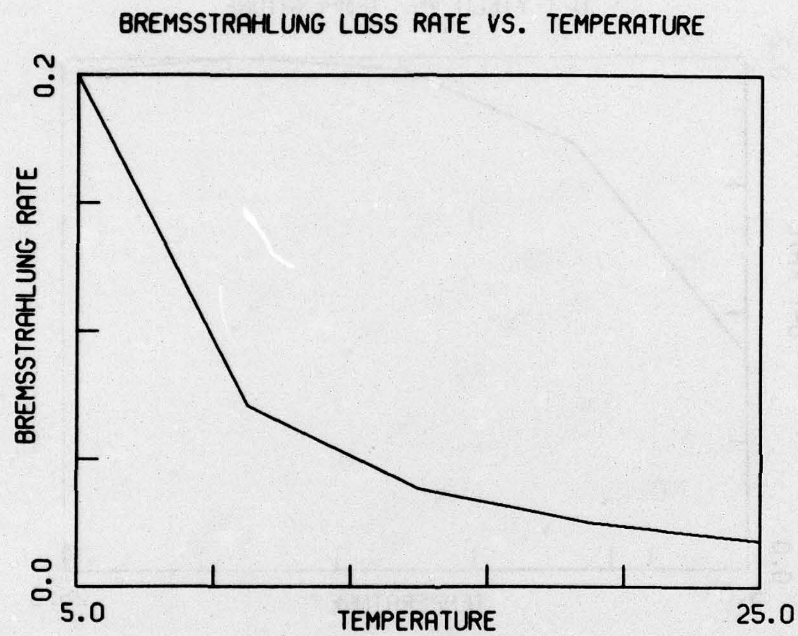

Fig. 10 — Bremsstrahlung rate as a function of temperature, scaled as in Fig. 9